KERNFORSCHUNGSZENTRUM

KARLSRUHE

Topography of π^--Irradiated Volumes

G. Büche

KERNFORSCHUNGSZENTRUM KARLSRUHE

KFK 2259

Institut für Experimentelle Kernphysik

Topography of π^--irradiated volumes

G. Büche

Topography of π^--irradiated volumes

Abstract. The charge exchange reaction $\pi^- p \to \pi^0 n$ and the
radiative capture of negative pions $\pi^- p \to n\gamma$ can be used
to control the range of π^- in matter like human tissue.
The calculations reported in this paper demonstrate that
it is possible to construct range monitors which allow the
radiation therapist immediate control of the π^- beam
setting with respect to the tumor volume. This monitoring
of range can be achieved from outside the body within short
times compared to irradiation times which are typical in
therapy.

Calculated probability distributions are reported of $\gamma\gamma$-
coincidences from π^0-decay as well as neutron-gamma
coincidences from radiative capture. The processes are
presumed to occur within a water phantom. The momentum
resolution of the beam, the detector geometry, neutron
scattering within the body as well as the influence of
converters on the reconstruction of the momentum directions
of γ-quanta have been taken into account. It turns out that
π^0 decay quanta can be used for range monitoring but not
for reconstruction of spatial π^- stop densities. The straight
neutron-gamma correlation, too, is suitable for monitoring
the range of negative pions.

Topographie π^--bestrahlter Volumina

Zusammenfassung. Die Ladungsaustauschreaktion $\pi^- p \to \pi^0 n$ sowie die Strahlungseinfangreaktion $\pi^- p \to n\gamma$ sind geeignet, die Reichweite von negativen Pionen z.B. in Gewebe zu überwachen. Für diese Reaktionen durchgeführte Berechnungen zeigen, daß Reichweiten-Monitore gebaut werden können, die dem Strahlentherapeuten gestatten, die tatsächliche Strahleinstellung bezüglich eines Tumorvolumens zu kontrollieren. Die Überwachung der Reichweite kann außerhalb des Körpers vorgenommen werden und in Zeiten, die kurz sind verglichen mit der Dauer von therapeutischen Bestrahlungen.

Es wird über Häufigkeitsverteilungen berichtet, wie sie für $\gamma\gamma$-Konzidenzen nach dem π^0-Zerfall und für Neutron-γ-Koinzidenzen nach dem Strahlungseinfang jeweils in einem Wasser-Phantom erwartet werden können. Die Impulsauflösung des Strahls, die Geometrie vorgegebener Detektoren, die Streuung der Neutronen im Phantom und der Einfluß der Konverter auf die Rekonstruktion der Impulsrichtung der γ-Quanten sind in den Rechnungen berücksichtigt worden.
Es zeigt sich, daß die Quanten aus dem π^0-Zerfall für die Überwachung der Reichweite, nicht aber zur Rekonstruktion der räumlichen Stoppdichte-Verteilung von negativen Pionen verwendet werden können. Die Korrelation von Neutron und γ-Quant aus dem Strahlungseinfang am Proton kann ebenfalls zur Überwachung der Reichweite ausgenutzt werden.

1. Introduction

The practical use of negative pions in radiotherapy
calls for a monitor system covering the range of these
particles in each individual case of irradiation. The
momentum distribution of the incident pion beam
determines the width of the stopping interval. Within
this interval the π^- are captured by atomic nuclei and
in most cases produce stars of strongly ionizing particles.
Therefore, it is this interval within the irradiated tissue
where cells get destroyed most efficiently. The range of
pions in tissue and bone can in principle be calculated.
However, energy degraders and different contents of chemical
elements in tissue as well as density variations have to be
taken into account.

Thus, at the beginning of every irradiation, one has to
make sure that the region to be irradiated has been
positioned correctly by the actual momentum setting of the
beam. The number of methods of range observation is limited
by the fact that during an irradiation procedure the tumor
zone will usually not be directly accessible to monitoring.
Therefore, the detectors have to be placed outside the human
body or a phantom.

Most of the particles generated after pion capture are
slowed down within the tissue. Only γ-quanta and neutrons
are able to escape from the body and their intensities can
be used for monitoring. The different reactions of pions
leading to gamma ray emission and suited for range control
were discussed some years ago (SPERINDE, TEMPLE, PEREZ-MENDEZ,
MILLER and RINDI 1971). To achieve spatial resolution within
the stopping interval, collimators should be used for most
types of quanta, such as mesonic x-rays or nuclear γ-rays.
In an experiment (SPERINDE, PEREZ-MENDEZ, MILLER, RINDI and
RAJU, 1970), where γ-quanta of energies greater than about
15 MeV have been detected with a wire spark chamber after
passage of a system of collimators, a spatial resolution of

6 mm has been obtained. The resolution was determined by the spacing of the lead plates in the collimator. In a second experiment (DEAN and HOLM, 1971) photons in the energy region from 100 to 200 keV have been detected with an ANGER camera. The authors have not specified the spatial resolution, that has been obtained.

For further development, scattering from the collimator system and finite penetrability of its laminae as well as energy resolution problems should be avoided as far as possible. Therefore, in the present paper, the interest has been concentrated on reactions that occur 'promptly' after the pion stops and that are spatially correlated by special decay kinematics. Such processes are initiated by the capture of negative pions in hydrogen.

$$\pi^- + p \rightarrow n + \pi^0 \qquad \text{(charge exchange)}$$
$$\rightarrow n + \gamma \qquad \text{(radiative capture)}$$

The kinetic energy of the neutral pion from the charge exchange reaction with protons at rest is 2.89 MeV. This energy is low and a neutral pion cannot travel a long distance during its lifetime of about 10^{-16} s. But its kinetic energy prevents the decay quanta from having antiparallel momenta. Therefore, the two γ-quanta may be used to evaluate the coordinates of the decay point from a measurement of the directions of their momenta.

Neutron and gamma-quantum originating from a radiative capture reaction have antiparallel momenta and definite energies. Therefore, they can be easily identified. However, because of their correlation angle of 180 degrees, one cannot reconstruct all coordinates of the reaction point. Nevertheless, they may be used at least for range monitoring.

In the next two sections of this paper calculations are reported on the intensity distributions from coincident events of the two reactions as a function of the detection geometry. In both cases, the sensitivities are given, that have been calculated for variations of the π^- range in a water phantom.

2. Topography using π^{o}-decay

If negative pions travel through hydrogeneous substances
like tissue, a small fraction of them undergo a charge
exchange reaction with protons. This is possible during
flight as well as after deceleration and capture into
molecular orbits. In the center of mass system of π^{o} the
two decay quanta have opposite momenta, but in the
laboratory system they include generally angles different
from 180 degrees. In addition to this angular correlation
in the decay of π^{o}, an angular distribution exists for the
generation process of this particle. Its angular distribution
in the laboratory system is isotropic, if π^{o}-particles are
generated after capture of π^{-} in hydrogen nuclei which are
constituents of molecules. But charge exchange reactions
occurring during flight show energy-dependent angular
distributions. The next three sections describe the facts
together with the assumptions that determine the distribution
of $\gamma\gamma$-coincidences from π^{o}-decay given in section 2.2 and
the sensitivity of a monitor system given in section 2.3.
These results have been discussed formerly in more details
(BÜCHE 1974).

2.1. Geometry of the detectors

To control the range of the negative pions using π^{o}-decay
two position-sensitive gamma ray detectors placed opposite
to each other are required. The detectors may be layers
of appropriate converter material installed in front of
multiwire proportional chambers. A cut through such a
schematic setup along the beam is shown in fig. 1.
At the entrance of the phantom, the beam may e.g. have an
energy E_{o}, a momentum resolution $\Delta p/p_{o}$, and a range R.
A definite element of the upper detector plane A is in
correlation with a linear chain of detector elements in the
other plane B.
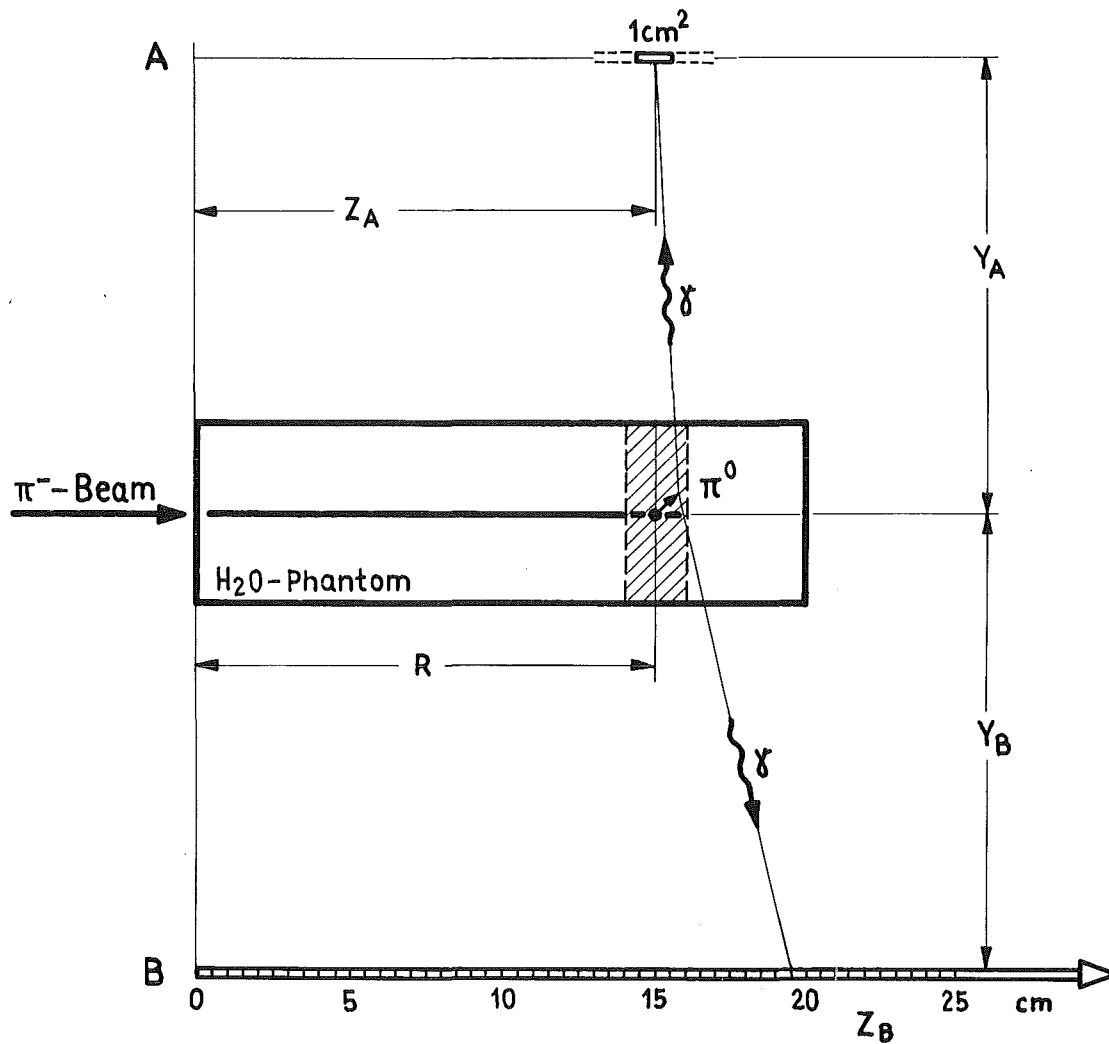
Fig. 1: Schematic setup for topography using the charge exchange reaction. A and B are two parallel planes of detector elements. They are cut vertical to their surface and parallel to the incoming beam.
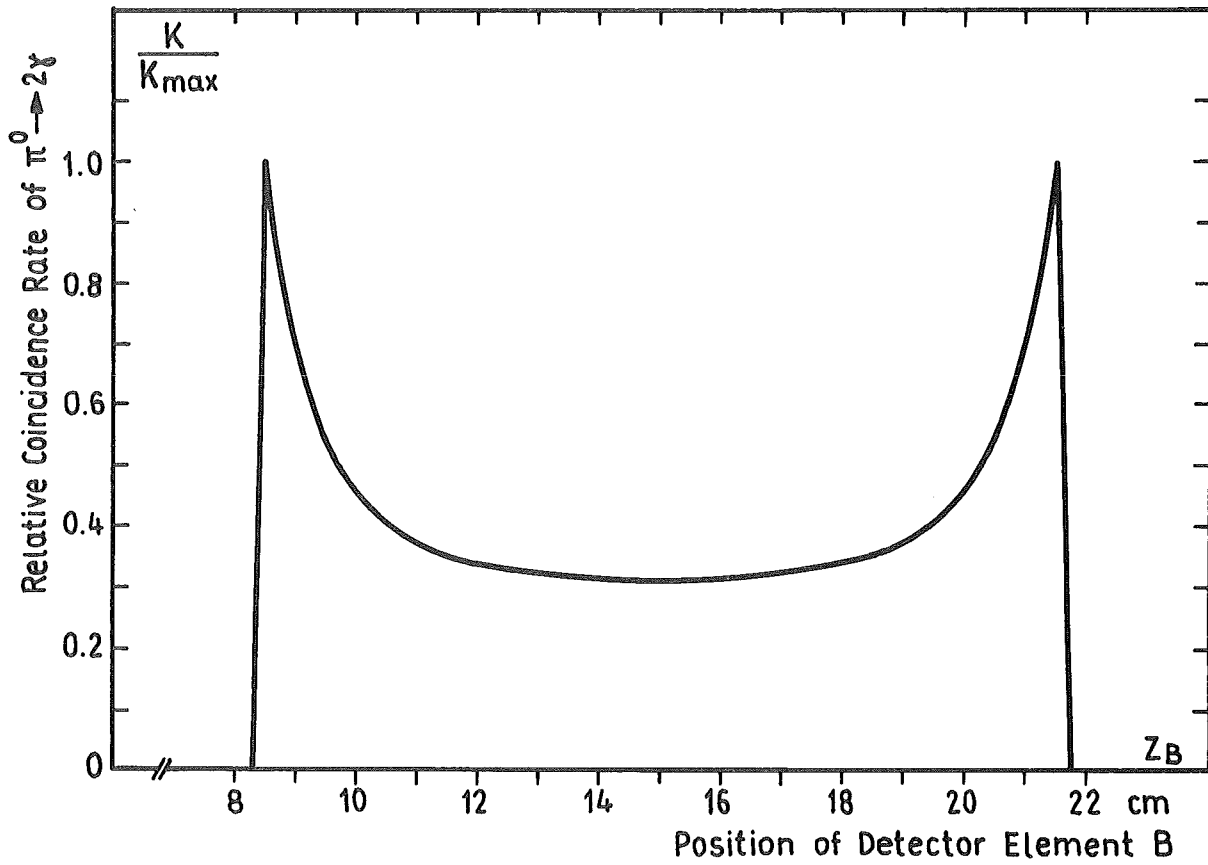
Fig. 2: Distribution of $\gamma\gamma$-coincidences K from
π^0-decay. One detector element is fixed
at $y_A(= - y_B) = 15$ cm; $z_A = 15$ cm.
All particles π^0 are generated from protons
at rest and emitted isotropically from the
point $y = 0$; $z = R = 15$ cm.

2.2. Distribution of coincidences

It has been assumed in a first step of the calculation
that charge exchange processes take place only at
positions with z = R and that there is no lateral
extension of the beam. Only reactions from water molecules
have been considered, where protons and π^- are nearly
at rest. The resulting distribution of coincident γ-
events as a function of the position of the detector
element within plane B is shown in fig. 2. As long as
the detector element A remains fixed at z_A = R, the
kinematical curve is rotationally symmetric about an axis
vertical to plane B. Therefore, fig. 2 shows a cross
section of this distribution with a plane containing
the element A and the z-axis.

To obtain the realistic coincidence curve, fig. 2 has
to be averaged over the range distribution of the π^-
beam. A zone of 2.5 g cm^{-2} has been evaluated for a beam
of E_O= 68 MeV and $\Delta p/p_O$= 6%. This momentum resolution produces a
range uncertainty which is much greater than that due to straggling.
In addition, charge exchange reactions occuring during
flight have to be considered. These reactions can take place
everywhere from the beginning of the water phantom until the
capture region where individual pions stop. The residual
energy of π^- as a function of their path length has been
calculated by integrating the expression for the energy
loss of BETHE and BLOCH. The appropriate cross sections and
angular distributions of the charge exchange reaction from
hydrogen has been evaluated on the basis of phase shift
analysis.

The results for the distribution of $\gamma\gamma$-coincidences are
given in fig. 3. The curve is composed of a broad continuum
determined by reactions occuring during flight and a
'volcano-like' distribution produced by the charge exchange
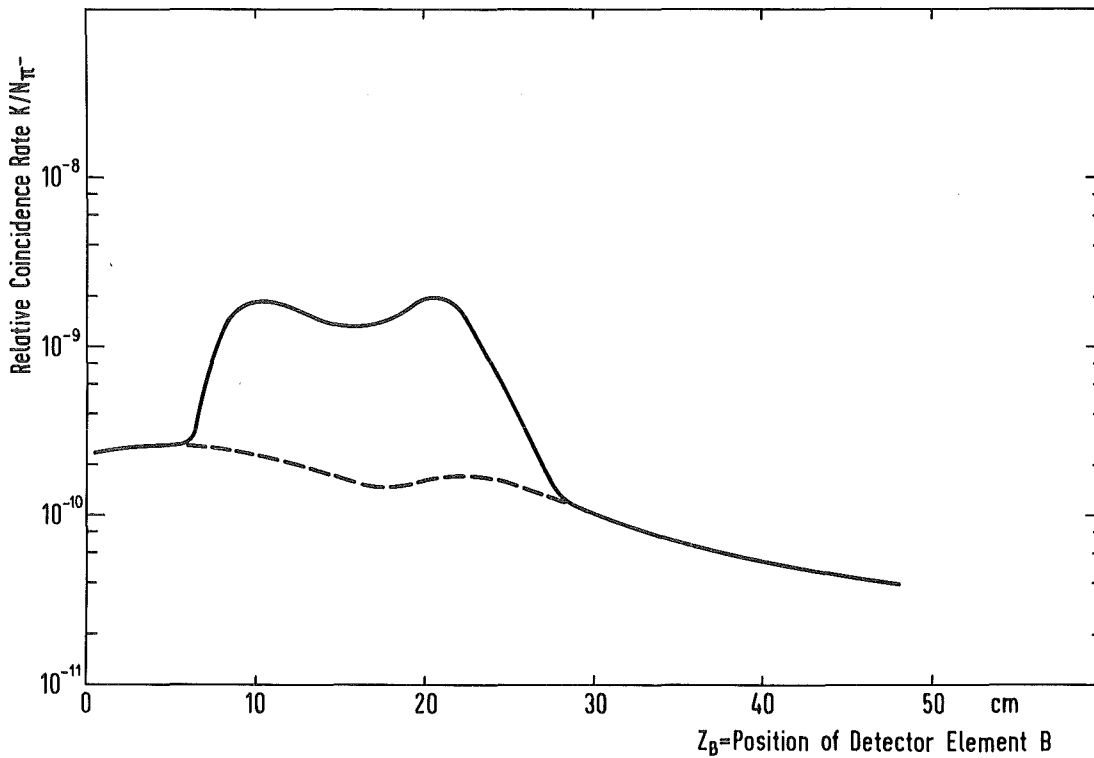
Fig. 3: The number K of $\gamma\gamma$-coincidences from π^o-decay within a water phantom calculated from the geometry of fig. 1 and related to the number $N_{\pi-}$ of incident π^-. The π^o are generated during flight as well as after complete deceleration. As in fig. 2, the detector element A remains fixed at $y_A (= - y_B) = 15$ cm, $z_A = R$ and has a sensitive area of 0.5×0.5 cm^2. Additionally, a stopping interval of 2.5 cm has been taken into account.

in the capture region. The position of this volcano-like distribution in the detector plane B is rather sensitive to the range of the beam. If the energy of the pion beam rises, the whole figure moves to greater values of z_B. Therefore, the counting rate from the detector elements situated within

the region of the greatest slope of the coincidence curve
is most sensitive to variations of the position of the
capture region. These detector elements within plane B
may be called 'sensitive' elements. Each detector element
in plane A has its proper distribution of coincidences for
elements in plane B. Therefore, the detector element A
together with its sensitive elements in plane B can be
shifted parallel to the beam within a certain region and
can be rotated around the beam axis. In this way, the
detector area A can be enlarged without noticeable loss
of spatial resolution.

2.3. Sensitivity of a range monitor using π^{o}-decay

The sensitivity of the system to changes of range is given
by the slope of the curve in fig. 3. At z_B = 7 cm one
deduces a sensitivity of $\left|\frac{1}{K}\frac{dK}{dz}\right| \approx 30\%$ cm^{-1} for one pair of
detector elements A and B and a value of coincidences
per π^- of K/N_{π^-} = 0.8 × 10$^{-9*)}$. While the element A remains
fixed, the element B can be enlarged by a factor of 20
with respect to the data of fig. 3 without an essential loss
of sensitivity. Independently, the element A can be moved
around the beam axis over half a cylinder of radius y_A and
15 cm height. These steps result in an enlargement of the
solid angle by a factor of V = 1.4 × 10^4 compared to one pair
of detector elements. A typical irradiation time for therapy
will be t = 10 minutes with a beam current of N_{π^-} = 5 × 10^7 s^{-1}.
If each γ-detector has an efficiency of η = 30%, one obtains
a number of coincidences of

$$K = (K/N_{\pi^-}) \cdot V \cdot N_{\pi^-} \cdot t \cdot \eta^2 = 3 \times 10^4$$

---

*) A fraction of 3.5×10^{-3} has been included for the number of
pions that undergo the charge exchange reaction
(PONOMAREV, 1973).

One standard deviation of this number of events corresponds
to a shift of 0.2 millimeters of the range of π^-. In other
terms, one tenth of a typical irradiation time is enough to
localize the stopping interval of the beam to an accuracy
of one millimetre. This method, therefore, permits the
stopping interval to be monitored by application
of a low dose compared to the whole dose necessary for
therapy.

2.4. Reconstruction of points where individual π^- stop

The two gamma-quanta from π^0 decay do not generally have
antiparallel momenta in the laboratory system. Therefore,
from the measurement of their points of detection, together
with the directions of their momenta, one can in principle
reconstruct the point of decay of π^0. To measure the
direction of momentum of the quanta, at least two position-
sensitive detectors one behind the other have to be provided
behind the converter. The reconstruction of the origin of
the correlated quanta largely depends on the conservation
of momentum direction during their conversion into electrons.
Electrons arising from Compton effect and pair production
and subsequent multiscattering within the converter introduce
deviations from the original direction of the momentum.
The following three figures illustrate the consequences of
these angular deviations. In each case layers of different
materials have been chosen that are equivalent with respect
to the conversion of γ-quanta into electrons.

If the electron and positron from pair production pass the
detectors at the same time, the center of their distance
should be defined as the point of event. Two events within
consecutive detectors define the reconstructed momentum
direction. For the calculation, the angular deviation from

the gamma direction of the reconstructed momentum direction
has been approximated by a Gaussian distribution. Its
standard deviation has been assumed to be equal to the mean
angle $<\theta>_{pair}$ between the electron-positron pair.
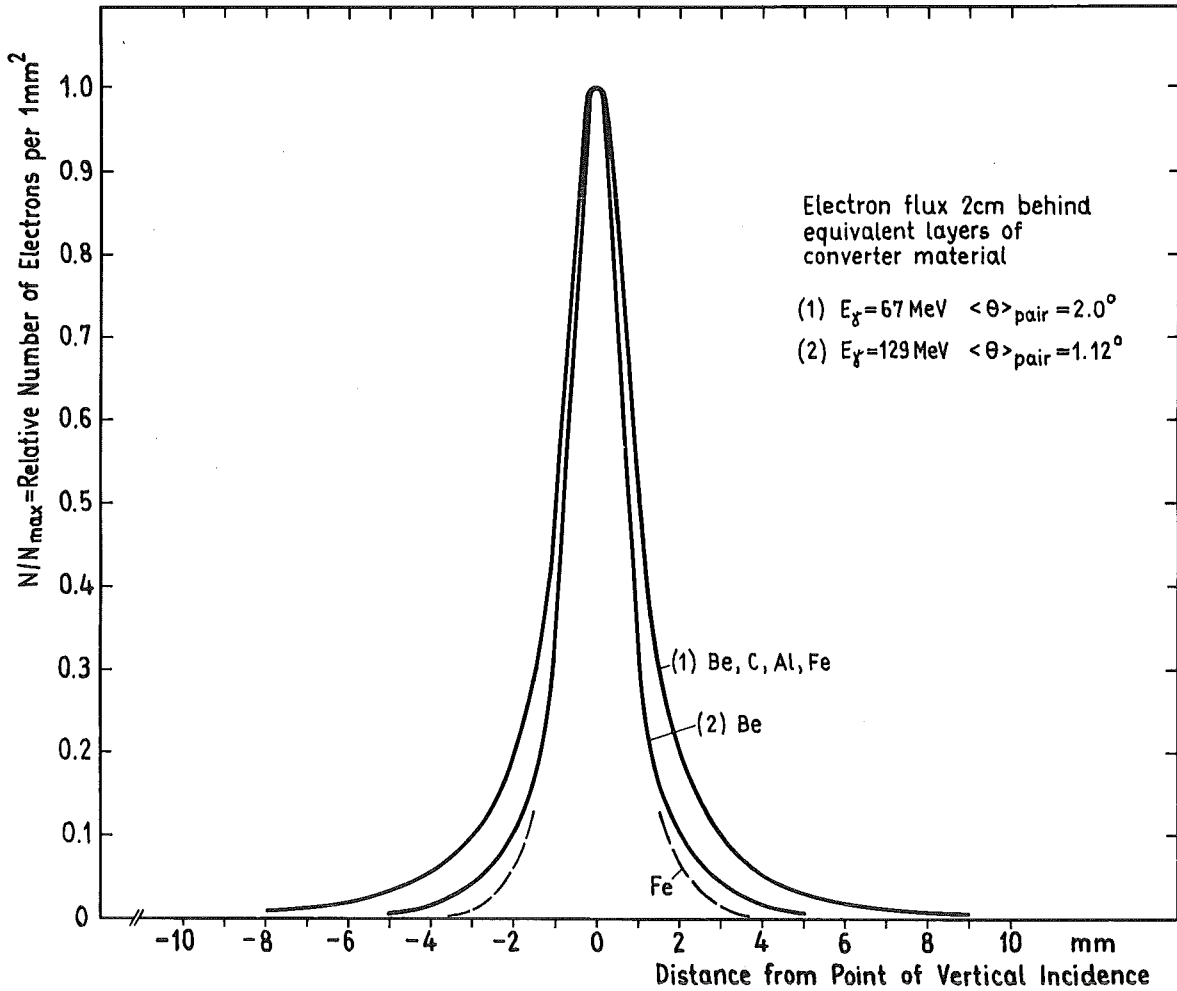
Fig. 4: Distribution of electrons hitting a detector
plane 2 cm behind the surfaces of γ-converters
with an efficiency $\eta = 0.07$. The quanta are
moving vertically onto the converter. The whole
figure shows rotational symmetry around the
momentum axis of the quanta. Curve 1: quanta from
π^{o} decay, curve 2: quanta from radiative capture.

Fig. 4 shows the relative number of electrons on a
position-sensitive detector as a function of the
distance from the point of vertical incidence of the
γ-quanta. The detector is assumed to be placed 2 cm behind
the surface of a converter having an efficiency of 7%.
The results of the calculation are:

(a) For gamma quanta of 67 MeV about 90% of all events
    deviate not more than ± 3 mm from the point of
    intersection of the incident γ direction.

(b) The atomic number of the converter material has
    only very little influence on the curves.
    Consequently, the conversion process has only little
    influence on the sensitivity $\left| \frac{1}{K} \frac{dK}{dz} \right|$ of fig. 3.

The coincident passage of one electron through two position-
sensitive detectors behind the converter defines a straight
line in space, along which the γ-quantum most probably was
moving before detection. These two lines defined by
coincident events intersect at the point where π^o has
decayed. But in general, these lines will not always
intersect because of the angular deviations previously
described. The only characteristic of these two lines
is their minimum distance apart. The centre of this section
represents the reconstructed decay point. This point has a
certain distance d from the actual origin of the two γ quanta.
Using Monte-Carlo methods, a certain number of events has
been reconstructed. Their distribution as a function of the
distance d from the origin is shown in fig. 5 for an angle
of 162° between the quanta and different converter materials.
In spite of the narrow geometry chosen for the detector elements
in coincidence, one observes a mean displacement of about 4 cm
of the reconstructed from the actual event. This mean dis-
placement increases to about 6 cm for an enlarged detector
geometry of y = ± 30 cm and z = 10 cm (see fig. 6, curves 1
and 2). The displacement even increases when the correlation
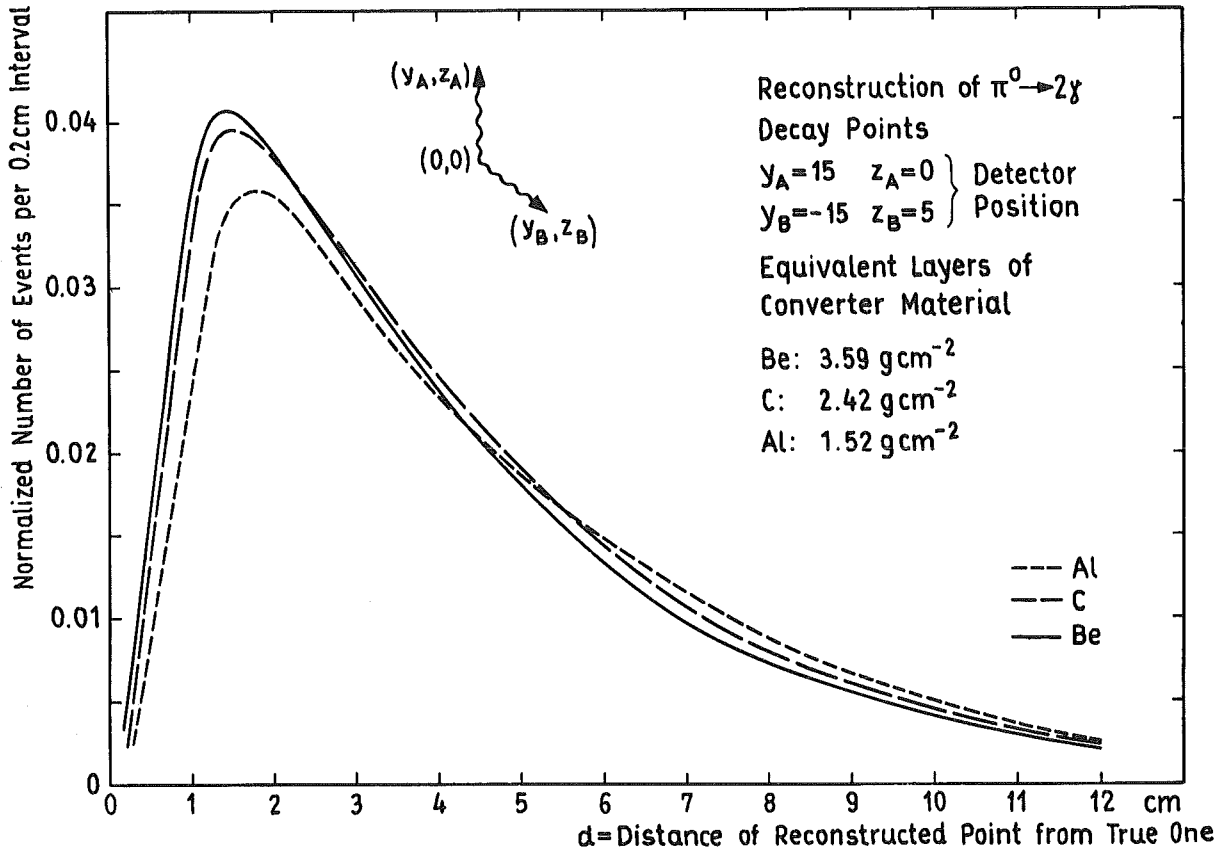
Fig. 5: Distribution of reconstructed π^o decay points.
The particles are assumed to decay at the origin
of the coordinate system and their γ-quanta are
detected according to fig. 4 behind equivalent
layers of converter material. The positions of
detection and the directions of momenta define two
straight lines in space. These lines do not intersect
generally, but the central point of their minimum
distance represents the decay point. Its distance
d from origin has been taken as abscissa.
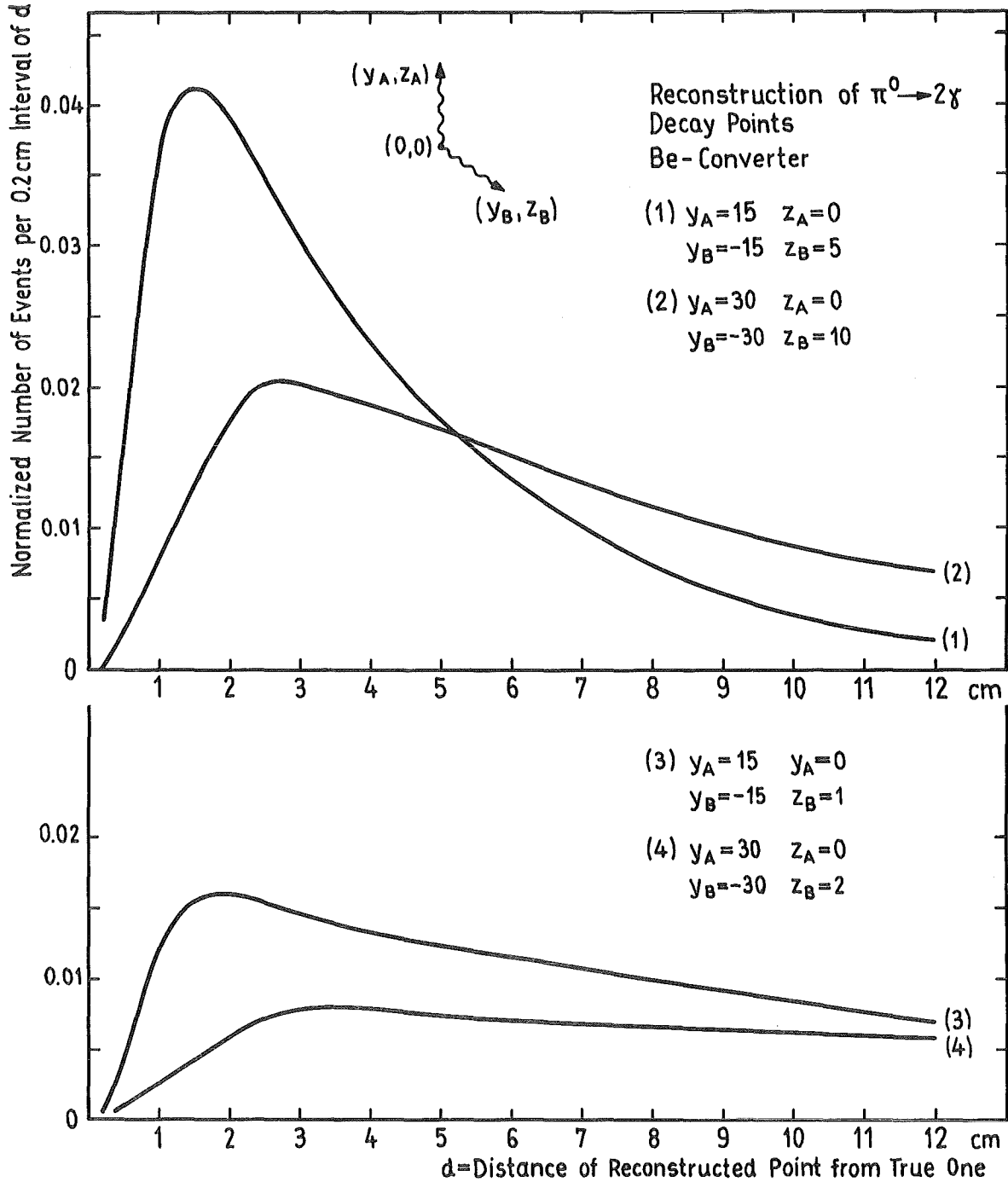
Fig. 6: Distribution of distances of the reconstructed decay
points from the true point as a function of the detector
geometry and the angle between the two gamma quanta.
For curves (1) and (2), the angle between the quanta is
fixed to 162°, for curves (3) and (4) the angle is 176°.
The relative probability of decay quanta showing these
angles can be taken from fig. 2 (A shift of 15 cm
should be taken into account for z_B).

angle for the two quanta tends to 180 degrees (see fig. 6, curves 3 and 4). For therapeutic conditions, distances of events between 4 and 6 cm from the origin seem to be too large to be used in practice. Therefore, on the basis of this calculation, the spatial reconstruction of π^- stop density within an irradiated volume does not seem feasible.

3. Topography using radiative capture

Besides the charge exchange reaction negative pions also suffer
radiative capture from protons. The relative intensities
are given by the PANOFSKY ratio. If the radiative capture
process occurs in pionic hydrogen within molecules, the
two particles in the initial state are nearly at rest. Then
neutron and γ-quantum in the final state are emitted with
antiparallel momenta. Therefore, neutron and γ-quantum in
coincidence can be used favourably to monitor the range of
negative pions. However, a correlation within a straight
line is sensitive to displacements of their origins in two
vertical directions only. Complete reconstruction of all
three coordinates is not possible without further new
information on the process. Such information may be the
direction of the momentum of the incoming π^-. However,
small angle scattering during the deceleration of pions
limits the spatial resolution.

3.1. Geometry of the detectors

A range monitor which uses a pair of particles with anti-
parallel momenta requires only a very simple detector
geometry with two detectors opposite to each other (fig. 7).
The neutron with an energy of about 9 MeV can be detected
with a plastic scintillator. Its energy can be measured
using the time-of-flight methods. The gamma quanta of
129 MeV can be detected by a thick NaJ(Tl) crystal. For
calculations the two detectors are positioned at points
with cartesian coordinates $(x, y, z) = (0, \pm D, 0)$ and the
point source coinciding with the origin. The sensitivity of
this setup to variations of range of π^- mainly depends on two
parameters: the diameters of the detectors and the extension
of the source, i.e. the stop region.
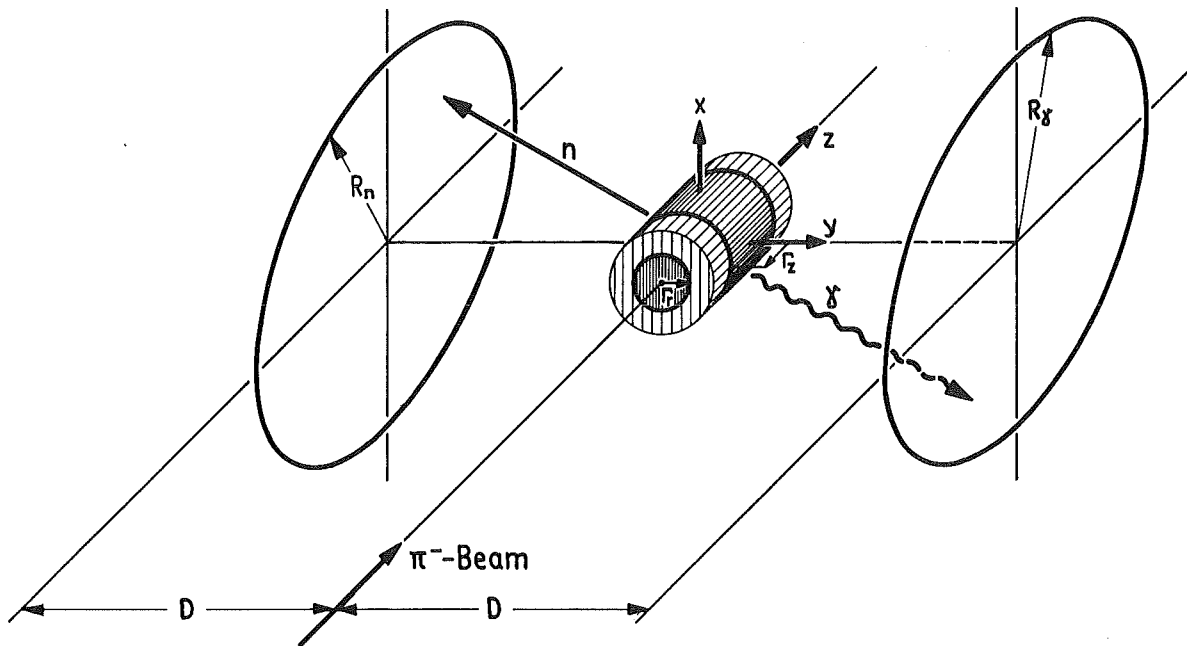
Fig. 7: Schematic geometry for range monitoring using
π^- radiative capture from protons at rest.
The beam extension is chosen axially symmetric
and the stopping interval is distributed around
$z = 0$. Γ_r and Γ_z are the standard deviations in
the Gaussian distribution functions accepted for
the radial extension and the stopping interval
of the beam.
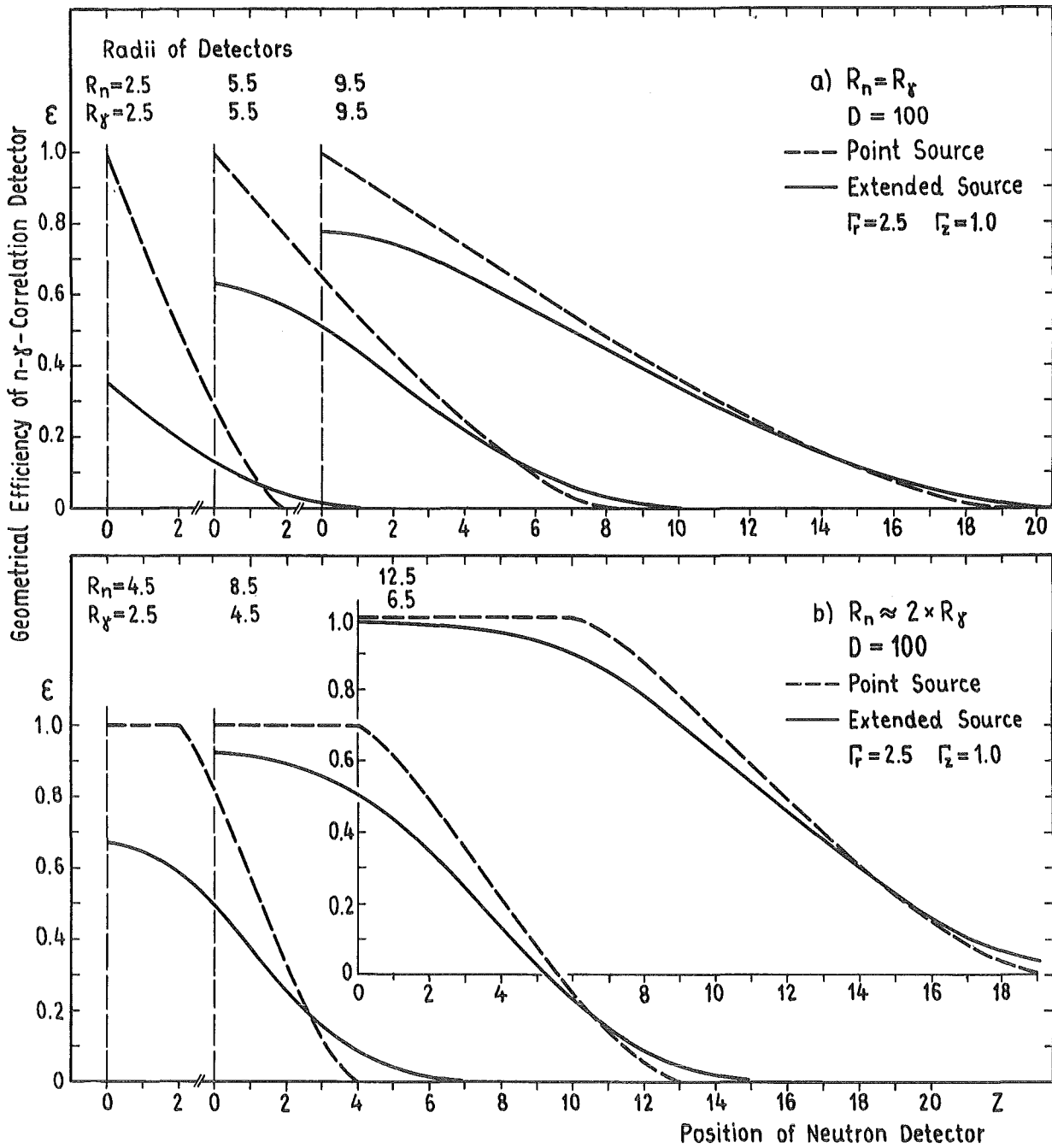
Fig. 8: Geometrical efficiency ε of a detector pair for neutrons and γ-quanta as a function of the position of the gamma detector. The parameters are the source extension and the detector size.

Fig. 8 shows the behaviour of the geometrical efficiency ϵ
if one of the two detectors moves parallel to the z-axis.
In each of the curves shown, a point source and an
extended source are compared. The extension of the stop
region has been approximated to a Gaussian
function with a full width at half maximum
$\text{FWHM}_z = 2 \; \Gamma_z \; \sqrt{2 \; \ln2}$. The same distribution function
has been chosen for the intensity within the beam cross
section (x,y-plane). For a fixed source extension and for
small detector diameters, ϵ is small, but the sensitivity
$\left| \dfrac{1}{\epsilon} \dfrac{d\epsilon}{dz} \right|$ is high. For large detector diameters the efficiency
tends to reach that of a point source, but the sensitivity
becomes low. It is obvious that detector diameters exist
for which both the sensitivity and the efficiency are
favourable for practical use. This statement applies to
detector pairs having equal as well as unequal diameters.

3.2. Scattering of neutrons within the phantom

Scattering processes of neutrons that travel through
tissue or phantom material may broaden the efficiency
curve and, therefore, have to be taken into account.
It follows from a rough calculation that only 22% of the
neutrons have not been influenced when leaving a layer
of 15 cm water. In water or tissue, the overwhelming number
of neutrons suffer from proton scattering. This scattering
is an elastic process as long as neutrons have energies in
the MeV region. Scattering from oxygen and other elements
occurs also via inelastic channels and is accompanied by
high energy losses which permit discrimination against
the elastically scattered neutrons. Neutron-proton
scattering is isotropic in the centre of mass system,
but has a maximum in the forward direction in the
laboratory system. These neutrons have lost only small
amounts of energy compared to inelastic scattering
from oxygen. A possible background count rate is then
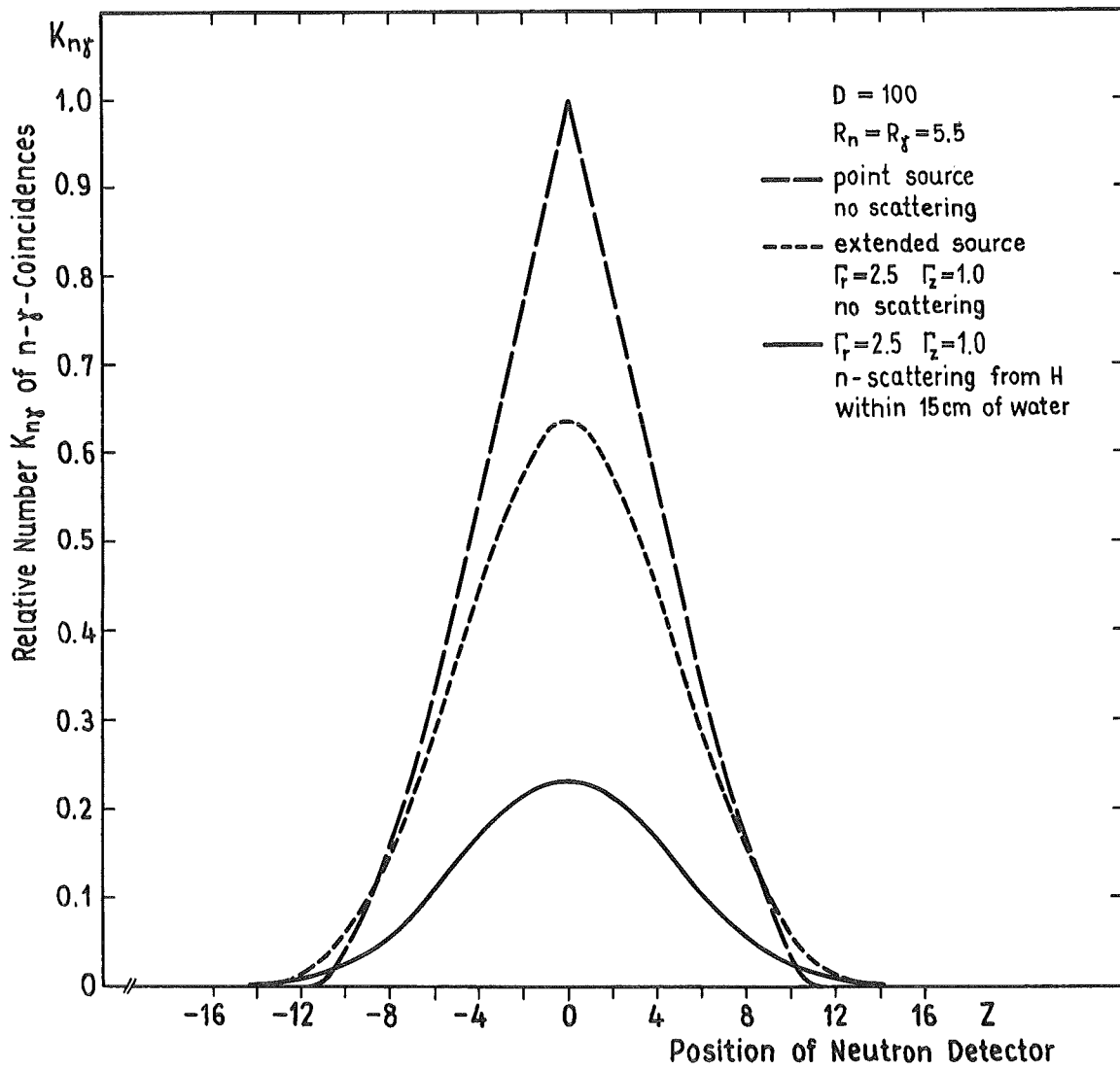
Fig. 9: Relative number of coincidences as a function of the position of the neutron detector calculated using Monte-Carlo methods. Neutron scattering from hydrogen within the water phantom has been taken into account.

increased and the sensitivity of the range monitor is lowered.

Fig. 9 illustrates the influence of neutron scattering. Only scattering from protons within 15 cm of water has been calculated. Reduction of coincidences to 36% of the value for an extended source, but no broadening of the curve is noticed. Therefore, the contribution of scattered neutrons, which show a smooth and very broad peak, does not substantially reduce the sensitivity.

The following two figures 10a and 10b illustrate the influence of different detector dimensions and source distributions on the coincidence curve including n-scattering. On the basis of fig. 8 a radius R = 5.5 cm for both the γ and neutron counters together with fixed D = 100 cm has been chosen as 'reference geometry'. Starting from this reference geometry (solid lines), fig. 10a shows the effect of unequal diameters for the solid angles with nearly no loss of sensitivity $\left| \frac{1}{K} \frac{dK}{dz} \right|$.

Fig. 10 b shows the influence from different source intensity distributions. The neutron detector may remain at a fixed displacement of about 5.5 cm in order to have maximum sensitivity in the reference geometry. Then the deformation of the coincidence curve going from a Gaussian distributed π^--stop region to a homogeneously distributed region is only of minor importance. But a homogeneously distributed cylindrical source of 10 cm diameter and 10 cm length lowers the sensitivity remarkably, even for detector distances as large as D = 1 m. Therefore, the reference geometry will be sensitive at least for dimensions of irradiated volume 5 cm in diameter and 5 cm in length.
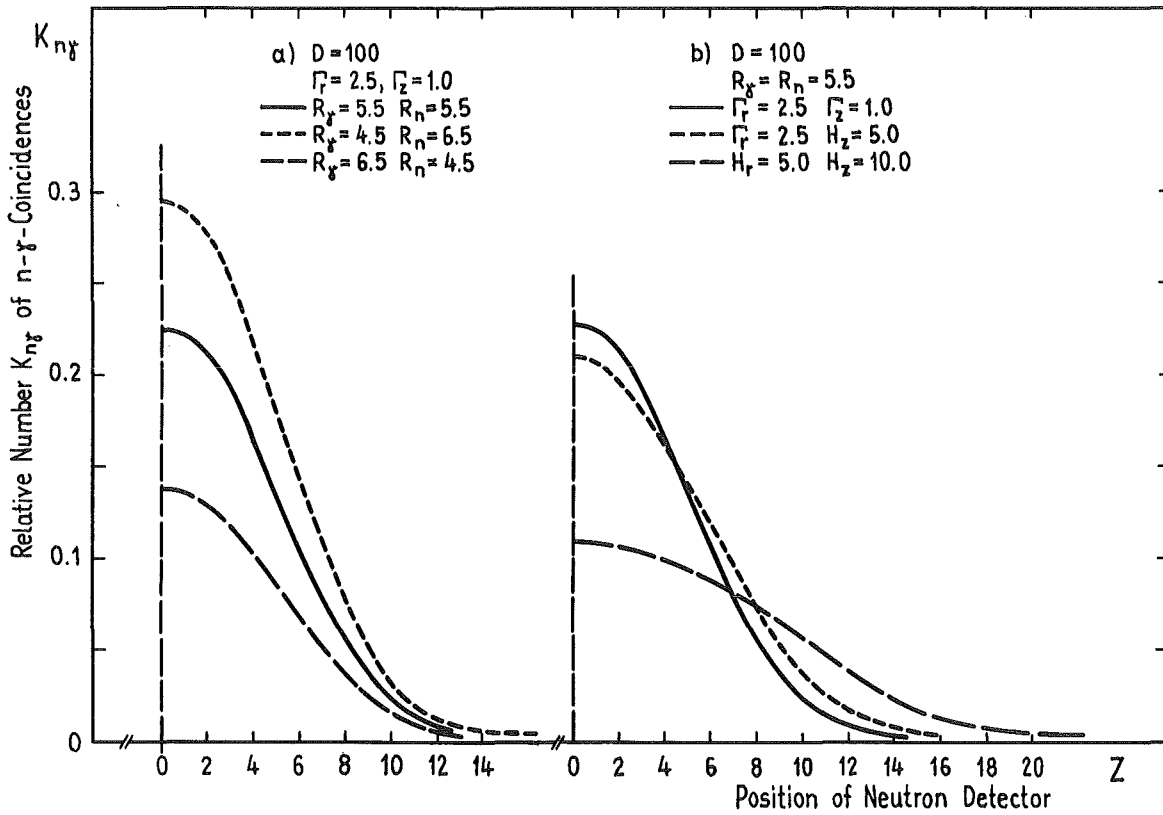
Fig. 10: Relative number of coincidences as a function
of the position of the neutron detector
calculated by means of Monte-Carlo methods.

a: source distribution fixed, different
detector sizes;

b: detector size fixed, different source
distributions. Γ is the standard deviation
of a Gaussian distribution, H is the width
of a homogeneous distribution.

Neutron scattering has been taken into account.

3.3. Sensitivity of a range monitor using n-γ-coincidences

The 'detector element' of a range monitor is the combination of one γ-detector and two neutron detectors that remain fixed in space on a certain radius D around the irradiated volume. The position of each neutron detector corresponds to one of the two points of greatest slope of the coincidence curve (see fig. 9, for example). If the stop region of pions has been positioned correctly, both detectors deliver the same number of coincidences with the γ-detector. If this is not the case, the difference of counts is a measure of the imperfectness of stop region positioning. The sensitivity of a typical range monitor element according to fig. 10 is about 23% cm^{-1} and the relative number of coincidences $K_{n\gamma}$ per γ-quantum N_γ detected is $K_{n\gamma}/N_\gamma \approx 0.14$. The relative solid angle for the γ-detector is 7.56×10^{-4}. Some ten or twenty elements can be positioned side by side around the phantom. In water, about 2.3×10^{-3} pions undergo radiative capture from hydrogen. A product of $\eta_n \cdot \eta_\gamma = 0.3$ can be accepted for the efficiency of the respective detectors. Then, for a beam current of 10^8 π^- s^{-1}, it takes about half a minute to count as much events as to allow control of the stop region within 1 mm. Therefore, a setup of this kind is able to serve as a range monitor for irradiations in radio-therapy.

4. Conclusion

Future applications of negative pions in radiotherapy
enable the therapist to cover the tumor zone with an
area of a highly effective particle flux. This zone is
almost identical with the stopping interval of the pion
beam. In every case of irradiation it must be guaranteed
that the volume in question has been positioned correctly
with respect to the momentum of the beam. Two different
reactions are suitable for construction of such a range
monitor system: charge exchange reaction and radiative
capture of π^- from protons. For each of the two cases
a counter setup for range control has been discussed
on the basis of calculations of the reaction kinematics
and the detection properties of the γ-quanta involved.
It results that both reactions are suitable for use in
a monitor system. According to the evaluated sensitivities
to displacements of the stopping interval the times
necessary for monitoring are small compared to a typical
irradiation time in therapy.

By contrast with range monitoring, the determination of
the stop density distribution over the irradiated zone
seems to be problematic. In the case of π^o decay the
complete reconstruction of all three coordinates of stop
points of individual π^- cannot be realized with sufficient
accuracy.

References
_____

BUECHE, G., 1974, Kernforschungszentrum Karlsruhe,
          report no. KFK 2062

DEAN, P.N. and HOLM, D.M., 1971, Radiat. Res. 48, 201

PONOMAREV, L.I., 1973, Ann. Rev. Nucl. Sci. 23, 395

SPERINDE, J., PEREZ-MENDEZ, V., MILLER, A.J., RINDI, A.
and RAJU, M.R., 1971, Phys. Med. Biol. 15, 643

SPERINDE, J., TEMPLE, L.E., PEREZ-MENDEZ, V., MILLER, A.J.
and RINDI, A., 1971, Nucl. Instr. & Meth. 97, 331